Journal of
Materials Chemistry A

Accepted Manuscript

This article can be cited before page numbers have been issued, to do this please use: Z. Tian, N. Fechler, M. Oschatz, T. Heil, J. Schmidt, S. Yuan and M. Antonietti, *J. Mater. Chem. A*, 2018, DOI: 10.1039/C8TA03213K.

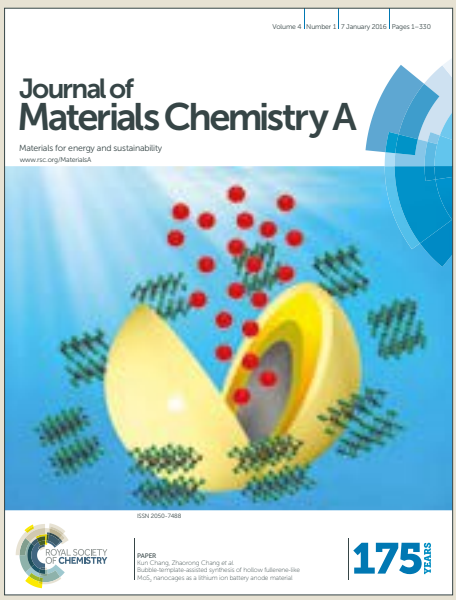

ROYAL SOCIETY OF CHEMISTRY

rsc.li/materials-a

View Article Online
DOI: 10.1039/C8TA03213K

Journal of Materials Chemistry A

ARTICLE

$C_2N_xO_{1-x}$ Framework Carbons with Defined Microporosity and Co-doped Functional Pores

Received 00th January 20xx,
Accepted 00th January 20xx

DOI: 10.1039/x0xx00000x

www.rsc.org/

Zhihong Tian,*[ab] Nina Fechler,[b] Martin Oschatz,[b] Tobias Heil,[b] Johannes Schmidt,[c] Siguo Yuan[a] and Markus Antonietti*[b]

Gallic acid and urea are used to produce C_2NO materials with rather dined micropores via direct condensation and ring closure. The materials show a unique heterocycle containing carbonaceous structure and features an unusually high content of heteroatoms (nitrogen, oxygen) lining inside the pores, meanwhile having high specific surface area. The multifunctional carbon materials demonstrate good performance for selective CO_2 capture resulting from the adjustable porosity and polarizability. In view of the simplicity of the salt flux synthetic method and the advantage of the available sustainable starting synthons, the C_2NO framework has potential for use in diverse practical applications.

Introduction

Microporous carbon materials with high specific surface area are key components in a wide range of fields, including adsorption,[1] gas separation,[2] electrocatalysis,[3] or in energy storage.[4] Such "designer carbons" with well-defined aromatization, heteroatom content, and pore architectures are mostly made by "carbonization", i.e. the simple heating of organic matter to very high temperatures, and this notation already indicates the little extent of bottom-up control in structure and functionalization provided by this process.

In our group, we published in the last years continued efforts to bring forward a more controlled, facile, sustainable, low cost synthesis of carbonaceous materials while being able to specifically control size and functionality of the pores. Especially a "C_2N"-species[5] which was simultaneously also described by the Baek group[6] is here to be discussed. The material, a porous, graphene-like structure in which 1/3 of all carbon atoms are replaced by pyrazinic nitrogen atoms (see also Scheme 1a) possesses a regular structure, have mostly a 12-atom sized circumvent, and the pores are lined tightly with basic nitrogen heteroatoms. Pores of related characteristics were shown in a recent paper to be "superhydrophilic", i.e. fill at relatively low partial pressures completely with liquid water.[7] In spite of a high structural porosity and similar to zeolites there are not unsaturated edge terminations, and especially there are no C-H bonds in the structure, justifying the understanding of these materials as "carbons" rather than as polymer frameworks. Interestingly, the species made as such seems to be thermodynamically rather stable, i.e. a whole range of carbonization recipes with very different educts (among them, beside cyclohexanehexone, also squaric acid/urea,[5b] thiooxamides,[8] and dihydroxychinon/urea[9]), result by spontaneous structural rearrangements in a similar final structure. This motif is stable up to 700 °C, then further graphitization sets in. As such carbons with dense and accessible hydrophilic micropores are exciting for a number of applications, including ion adsorption,[10] removal of polar gases,[11] or electrocatalysis,[12] it is the purpose of the present work to generalize the previous work and describe a cheaper and flexible route towards similar systems based on naturally abundant or Nature-derived starting materials. The involved "design rules" were recently described in a concept paper[13] and involve monomer prealignment and directional, "click-like" organic reactions to constitute heteroatom containing functional tectons with medium-high stability.

The intended generalizations concerns two aspects:

- We want to move from rather elaborated synthetic educts to more simple, more available, and sustainable starting synthons, here gallic acid and urea as a nitrogen source.
- We want to extend the previous pyrazine functionalization to related, easy-to-bridge heterocycles, namely oxazines and dibenzodioxines. The corresponding (idealized) frameworks with their heteroatom lined pores are depicted in Scheme 1b.

It is well known that introduction of other elements such as nitrogen or oxygen into the carbon lattice greatly enhances materials properties in terms of chemical and thermal stability, band positions, catalytic efficiency, improves significantly oxidation stability[14] and contributes to more specific interactions with liquids, solvated ions, or gases.[15]

[a] School of Materials Science and Engineering, Zhengzhou University, Zhengzhou 450001, P. R. China. *E-mail: zhihong.tian@mpikg.mpg.de.
[b] Department of Colloid Chemistry, Max Planck Institute of Colloids and Interfaces, Potsdam 14476, Germany. *Email: office.cc@mpikg.mpg.de
[c] Technical University of Berlin, Institute of Chemistry, Hardenberg str. 40, 10623 Berlin, Germany.

† Electronic Supplementary Information (ESI) available. See DOI: 10.1039/x0xx00000x

View Article Online
DOI: 10.1039/C8TA03213K

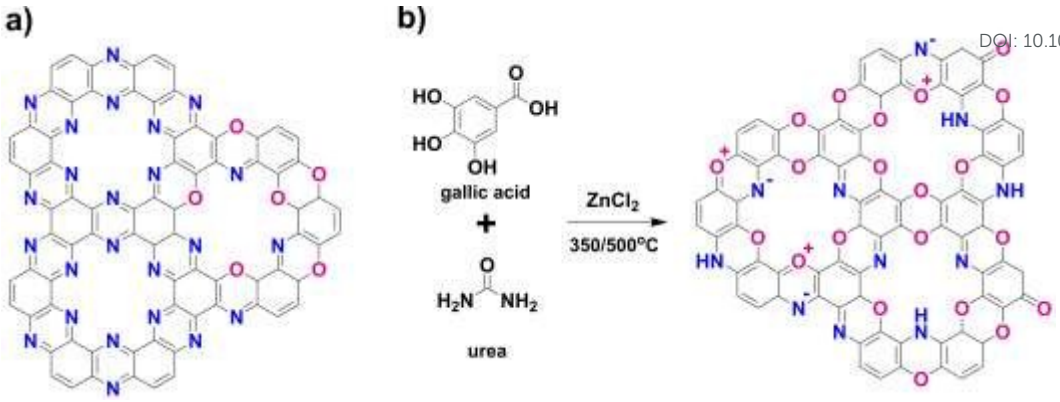

Scheme 1a: Idealized structure of 1,4 "dual doped" carbons, i.e. pyrazine, oxazine, and dioxine containing frameworks. Note that in this structural idealization, all heteroatoms are used for the most stable edge termination of a graphitic sheet, 33 mol% of all atoms are either N or O and all heteroatom substituents are in para position to each other. **Scheme 1b:** Using urea, a pure "$C_2N_xO_{1-x}$" structure as we expect to form. The structure depicts a reduced version, as the products are electroactive.

In this work we show that the resulting heteroatom doped carbon materials (ideally with about 33 mol.% heteroatom doping, i.e. every second ring has to host 2 heteroatoms, energetically preferred in para position to each other) are unusually polar, electrochemically active, and constitute a new type of carbonaceous sorbent with high sorption strength, e.g. to CO_2 ,and thus capacity under relevant conditions. Due to the predominant para-character of the substitution patterns, all doping centers can easily electronically communicate with each other, and the novelty to be expected as compared to classical heteroatom doped carbons comes from the fact that the heteroatoms are in particularly attractive mutual arrangement and thus carbon properties are altered by the concerted action of at least two doping atoms.

Results and discussion

Gallic acid is used as the primary starting product as shown in Scheme S1. It is a well-known natural resource and found in gallnuts, witch hazel, tea leaves, sumac, oak bark, and other plants. Gallic acid is well known to decarboxylate at higher temperatures to result pyrogallol[16], i.e. the carboxylic acid unit can be seen as a "protecting/leaving group" to enable a controlled substitution chemistry to realize the high structural definition.

As an entry scheme for more effective functionalization, we use the addition of urea and three well-known chemical reactions, which were found to occur simultaneously throughout the monomer condensation:

- Urea decomposes at around 130 °C under the formation of ammonia and isocyanic acid, which both act as linkers.[17] Isocyanic acid undergoes spontaneous isocyanate formation with oxygen nucleophiles such as the phenolic groups.
- Aromatic OH-groups can conveniently be turned with amines into -NH_2 substitution patterns, using Lewis acid catalysis.[18] Urea indeed serves as a convenient and sustainable ammonia source at elevated temperatures (see first point and Scheme S1).
- Gallic acid condenses with aromatic amines to oxazoles in a highly defined fashion, as for instance well known from the synthesis of gallocyanines[19] After formation of the central oxazole ring, the structure even more easily decarboxylates, allowing further substitution on the pyrogallol ring. It is exactly this simple heterocyclic reaction coupled to consecutive liberation of the carboxylate as a "protection group" for the 4 position which makes to our opinion gallates rather favorable starting products for extended 2-d para-heteroatom-doped carbons via a polycondensation scheme. Interestingly, gallocyanines as the related, low molecular weight dyes are black in the solid state, i.e. they have an appropriate electronic structure of a narrow bandgap semiconductor already in their molecular crystals.

Condensation occurs mainly along these expectations. When forming a liquid eutectic mixture of gallic acid, urea, and molten $ZnCl_2$ as a catalyst and solvent, spontaneous foaming via excessive CO_2 formation but no release of ammonia is found to occur at around 100 – 120 °C. The observed mass loss goes well with the decarboxylation of gallic acid plus release of a larger extent of the CO_2 of urea by transamidation, isocyanate formation and hydrolysis due to the added Lewis acidic $ZnCl_2$. In this stage, the reaction rapidly increases viscosity due to the ongoing polymerization processes, then the reaction gels, which clearly proves the ability of the monomers to be involved in branching reactions, and finally turns resin like, due to a high extent of multidimensional polymerization and cross-linking. This all occurs well ahead of any onset of carbonization and resembles typical urethane foam formation. The $ZnCl_2$ fluxes act as catalyst and solvent to promote the condensation reaction and later as porogens throughout the condensation processes, in which the obtained material is mechanically stabilized against shrinkage. The obtained carbons are referred to as GU11-Y, GU12-Y and GU13-Y, with 11-13, Y signifying the molar ration of gallic acid

View Article Online
DOI: 10.1039/C8TA07317K

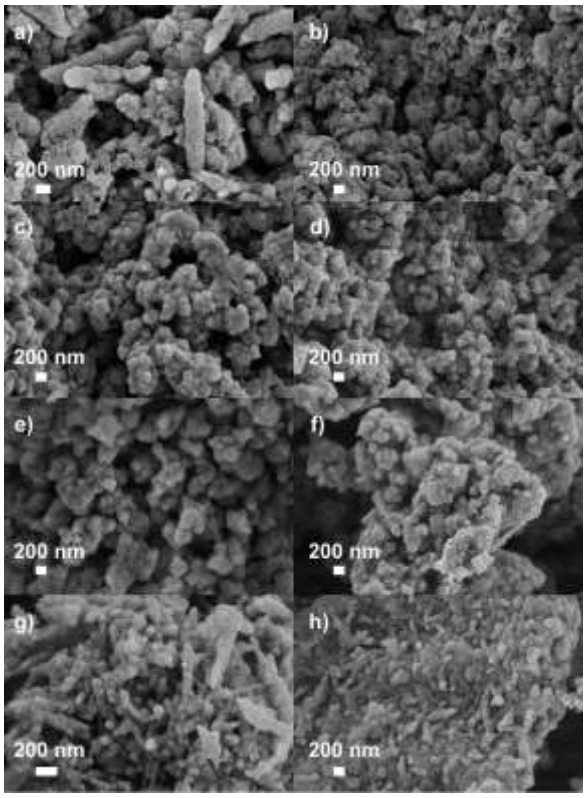

Fig. 1. SEM images of a) G-350, b) GU11-350, c) GU12-350, d) GU13-350, e) G-500, f) GU11-500, g) GU12-500 and h) GU13-500.

to urea and Y being the condensation temperature, respectively. G-Y is urea-free carbon obtained solely by condensation of gallic acid.

This condensation process is based on the elimination of carboxyl, hydroxyl, carbonyl and amine groups in the carbons. We used FT-IR measurement to probe the nature of functional groups on the carbons (Fig. S1). The FTIR spectra of both the 350°C and 500°C carbons show rather broad signals with low intensity, confirming the high degree of condensation already at comparably low temperature.[20] The carbonaceous nature is also supported by Raman spectra of the GU13-350 and GU13-500 (Fig. S2). A sharp G band was observed at 1591 cm^{-1}, and the D band usually assigned to the defects was found at 1359 cm^{-1} which is generally taken as the presence of a disordered graphitic lattice. We confirm that both the 350 °C and 500 °C carbons are very stable by performing thermogravimetric analysis (TGA) on the samples in air (Fig. S3). The samples without urea tend to decompose earlier, manifesting that nitrogen doping further enhances the oxidation resistance. The 500 °C series (burn off maximum: 500-600 °C) show higher thermal stability than 350 °C series (burn off maximum: 400-550 °C). This is due to the well-defined framework, which is fully developed in the 500 °C samples.[21] Compared with standard activated carbons,[22] the dual-doped carbons in this work have higher thermal stability. i.e. oxidize at higher temperatures owing to the large amount of O and N inside their structure.[23] The samples decompose/oxidize leaving almost no residual mass at 700 °C. Such a high temperature needed for complete decomposition is very unusual for other carbonized materials, but typical for regular, thermodynamic stable materials where a clear decomposition chemistry can be assigned.[14] The complete mass loss also indicates the absence of Zn residuals independent of the synthesis temperature and the urea content.

The elemental compositions of the condensation products as determined by combustion elemental analysis are summarized in Table S1. Especially when performing the reaction with Gallic acid: Urea in a 1:3 mole ratio in the presence of excess salt, the system is indeed nearby a composition with 2/3 carbon atoms and 1/3 doping heteroatoms, e.g .the structure of GU13-350 is $C_2O_{0.7}N_{0.2}$, the one of GU13-500 is $C_2O_{0.5}N_{0.2}$, i.e. we observe a minor extend of C-C condensation on top of the targeted reaction cascades. At 500 °C condensation, we still found a similar material, but with less hydrogen and a slight excess of carbon when compared to nitrogen and oxygen, i.e. the doping atoms get eliminated in amounts of a typical side reaction.

As typical for such materials, further increase of condensation temperature to 800 °C and 900 °C under inert gas leads to more extended carbonization within the structure and the destruction of the "para-dual doping motif" as such. In consequence, the N content decreases with the increase of temperature. The amount of N and O remaining after condensation at 800°C and 900°C is however still in between 24-25 and 20-21 wt%, Based on our experience, we would fix the thermal stability limit of heteroatom lines pores similar to those presented in Scheme 1 to 700 - 750 °C.

The textures of the samples were then firstly analyzed with SEM, the data are presented in Fig. 1. All powders have rather defined nanostructures with a primary grain size of 50 – 200 nm, i.e. too high contributions of an external surface area to interface properties are not to be expected. The powders are also rather well packed on the secondary hierarchy level, and

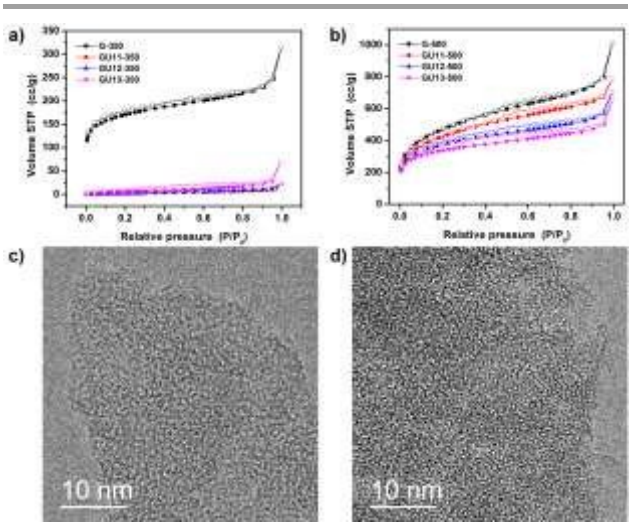

Fig. 2. a), b) N_2 adsorption (solid symbols) and desorption (open symbols) isotherms at 77 K for the C_2NO-frameworks obtained at 350 °C and 500 °C. HR-TEM of c) GU11-350, d) GU11-500.

View Article Online
DOI: 10.1039/C8TA03213K

Table 1. Textural properties of samples.

Sample	S_{BET} (m^2 g^{-1})	S_{mic} (m^2 g^{-1})	V_t (cm^3 g^{-1})	V_{mic} (cm^3 g^{-1})
G-350	627	448	0.49	0.19
GU11-350	11	2.9	0.03	0.002
GU12-350	4	0	0.03	0
GU13-350	17	0	0.1	0
G-500	1699	678	1.57	0.37
GU11-500	1532	669	1.22	0.35
GU12-500	1339	742	1.09	0.36
GU13-500	1227	791	1.02	0.35

S_{BET} calculated from nitrogen adsorption isotherms (77 K) by the Brunauer-Emmett-Teller method. V_t: total pore volume at $P/P_0 = 0.995$. V_{mic}: Cumulative DFT pore volume (<2 nm).

we specifically can exclude one or two dimensional character of the primary particles which would lead to a different texture.

Nitrogen physisorption was employed to study the inner specific surface area and pore size of the obtained condensation products (Fig. 2ab, Fig. S4), the corresponding quantitative data are summarized in Table 1. The urea-containing samples condensed at 350 °C have only minor porosity accessible for nitrogen, and the low values found are those which can be related to the outer texture seen in Fig. 1. The sample without urea possesses the highest porosity, predominantly microporous. At 500 °C, a high porosity and specific surface area (SSA) has developed. Higher contents of urea result in a relative stronger contribution a well-defined microporosity and less mesopores, which we attribute to higher fluidity of the reaction mixtures and a more lined character of the structural micropores. In order to shed more light on this process of pore formation, GU13-400 and GU13-450 were prepared along the same recipe as GU13-350 and GU13-500, but at 400 and 450 °C, respectively. The amount of nitrogen adsorbed at 77 K, shows a gradual increase as the condensation temperature changing from 350 to 500 °C (Fig. S5). This is accompanied by a growth of the micropore volume while keeping the sorption curve rather similar, i.e. more and more micropores become accessible for the adsorbate molecules. We attribute this process to the removal of pendant functional groups and the formation of phenazines, oxazine or dioxine rings through ring closure during the controlled condensation process. i.e. the still polymeric aromatic precursor system stack together before 350 °C, but the relevant organic rearrangement and the opening and stacking of closed 12-atom lined pores start to set in at 400 °C and is completed at 500 °C. Therefore, the porosity of the well-defined 1,4 dual doped carbons mainly comes from the formation of the holes surrounded by completed and closed aromatic rings in the materials' skeleton, i.e. the pores are tectonic and not due to bonding or packing defects.

The Brunauer-Emmett-Teller (BET) specific surface areas (hereinafter referred to simply as surface area) at 500 °C lies between 1200 and 1700 m^2 g^{-1}, depending on urea content, and thus exceeds zeolites and even most hierarchical zeolites.[24] This is expected, as with similar pore size and wall thickness a carbon as compared to a silica has a lower mass density. Please note that the nitrogen surface areas of all 350 °C samples are significantly lower than the samples at 500 °C which we attribute to a worse accessibility of the internal pore volume, as it will be shown below with CO_2-sorption experiments. With increasing the condensation temperature from 350 to 500 °C (Table S2), the surface area raises from 17, 46, 595 to 1227 m^2 g^{-1} for sample GU13-350, GU13-400, GU13-450 and GU13-500, respectively. The pore volume follows a similar trend, rising from 0.1 cm^3 g^{-1} for GU13-350 to 1.02 cm^3 g^{-1} for GU13-500. The surface area drops again with higher temperatures (650-900 °C), which can be attributed to the disintegration of the oxygen rich framework. A condensation temperature of 850 °C yields GU13-850 where the specific surface area decreases to 1167 m^2 g^{-1} (Fig. S6). In general, further increase of temperature leads to pore collapse (with the interface energy being the driving force) and the formation of lower surface area carbons as the walls are getting thicker, slowly moving the system towards more extended graphene units and more pronounced aromatic stacking in the walls.

Since low pressure nitrogen physisorption measurements in such polar materials can suffer from the high quadrupole moment of nitrogen and thus results in large errors in the determination of the micropore size we carried out argon physisorption at 87 K in order to determine the micropore size exemplarily for sample GU13-500 (Fig. S7). The shape of the isotherm is comparable to the measurement with nitrogen as the adsorptive, and the average size of the micropores for the GU13-500 is 1.45 nm.

Water vapor adsorption at 298 K (Fig. S8) was carried out on the GU13-350 and GU13-500 samples in order to investigate

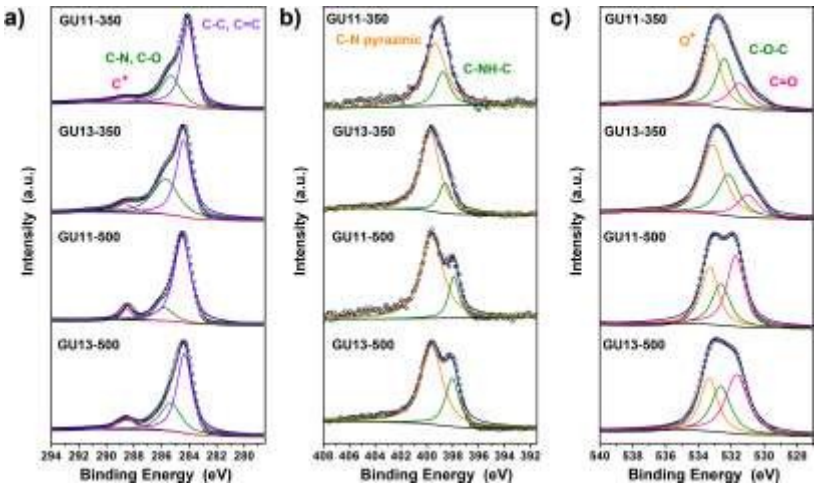

Fig. 3. Deconvoluted XPS spectra of the carbons: a) C 1s, b) N 1s, c) O 1s.

the strength of water adsorption which is a particular feature of zeolites. Both isotherms show significant uptake of water even at very low relative pressures. Such a strong interaction of the carbon pores with water does not take place in classical porous carbons even if they contain very narrow micropores. These measurements indicate the presence of strong water binding sites in our carbons, very much as in zeolites. In accordance to the nitrogen physisorption experiments, GU13-500 has a higher overall water uptake as compared to GU13-350 according to its higher pore volume.

The powder XRD pattern of the 350 °C carbon showed a broad feature cantered at $2\theta \approx 26^{o}$ (Fig. S9a), which is usually attributed to the stacking of aromatic systems.[25] The degree of stacking is not pronounced. Interestingly, this peak practically vanishes as the condensation temperature increases to 500 °C (Fig. S9b), which means that very little layer packing is present in all the samples. It is known from aromatic systems with dioxine bridges that can be easily bent, and even stable transversal rings can be created. The absence of graphitic packing is supported by high resolution transmission electron microscopy (HR-TEM). As shown in Fig. 2d, no obvious graphitic domains are observed, but rectangles were found to cross each other, like in a fiber fabric.

XPS measurements were employed to identify the chemical composition in the different materials (Fig. S10). In agreement with the combustion analysis (in which some adsorbed water may contribute to the detected oxygen especially in the urea-rich samples), XPS elemental analysis proves the high heteroatom content in the materials (Table S3). The C 1s peak (Fig. 3a) shows mainly three types of C. The primary peaks at 284.3 corresponds to C-C, C=C and C-H species, followed by peaks at 285.7 for C-N and C-O. It is worth mentioning that the peak at 288.7 (usually attribute to highly oxidized carbon or a C^{+}) is created throughout the process of condensation, and this peak becomes bigger with more urea. We cannot exclude the presence of carboxylates or even very strongly adsorbed CO_2, but it is to be mentioned that such electron poor carbons also exist in multiply heteroatom doped aromatic systems. The N 1s region of the spectra can be deconvoluted into two peaks (Fig. 3b). The binding energy at 398 eV is generally assigned to a secondary amine in the para position of oxygen. The other one with a higher binding energy of 399.5 eV can be attributed to nitrogen in aromatic rings, i.e. pyridines, pyrazines, and oxazines. The high intensity of this peak suggests a high proportion in six-membered aromatic rings. Together with the overall very high heteroatom content of about 30 mol%, these results indicate that N is integrated into the carbon framework most presumably in the para position with a second heteroatom. Peaks for O 1s are found for all samples at 531.4 and 532.5 eV corresponding to C=O and C-O-C, respectively (Fig. 3c). Another interesting finding is that peaks which correspond to O^{+} for O 1s were observed at 533.3 eV. Similar to many dyes in nature e. g. methylene blue and anthocyanin, our synthesis scheme based on gallic acid and urea gives aromatic systems which are conjugated throughout the oxygen atom, localizing a formal (+)-charge at this heteroatom position.

Considering the combination of high heteroatom content, predominant 1,4-para dual heteroatom doping and a well-defined, high specific surface area induced by the employed unique chemical condensation motifs, the samples were tested in CO_2 sorption experiments to determine their selectivity. As we pointed out in a recent review article, suchlike materials will be very attractive for selective CO_2 capture at low pressure because a strongly polarizing surface is much more important than a high nitrogen surface area and carbon dioxide uptake at 1 bar.[2a] In ideal case a material suited for this purpose would combine notable CO_2 adsorption with kinetic exclusion of nitrogen. The data are summarized in Fig. 4, Fig. S11.

Ordinary microporous activated carbons are known to possess only low IAST CO_2/N_2 selectivity in the range of 5-20, as the polarizable conjugated graphitic carbons bind many molecules based on the rather non-selective polarization resulting from van-der-Waals interactions.[2a] In consequence, this is how our highly porous but non-nitrogen-doped sample G-500 is performing (Fig. 4c). As compared to that, the sorption behavior of the N,O-dual doped carbons only has little in common with ordinary carbonaceous materials. The selectivities are rather high for both the 350 and 500 °C samples prepared with urea. While it is widely accepted that (even rather random) heteroatom doping as such can significantly enhance CO_2/N_2 selectivity by introducing specific binding sites inducing strong polarization of CO_2 (typical values of N-doped carbons with comparable nitrogen content are in the range of 20-40),[11a, 26] the polarization of CO_2 is apparently even stronger in our well-defined 1,4 dual doped materials and their selectivity of 67.5 (GU13-350) and 50 (GU13-500) are indeed approaching the values which are typical for performance separation products.

View Article Online
DOI: 10.1039/C8TA07217K

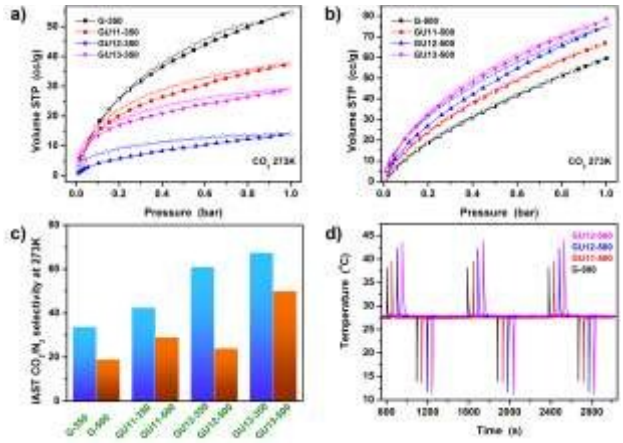

Fig. 4. a), b) CO_2 adsorption (solid symbols) and desorption (open symbols) isotherms at 273 K for the materials prepared at 350 °C and 500 °C. c) CO_2/N_2 selectivity as calculated by the IAST method for a CO_2:N_2 = 0.15:0.85 gas mixture at 273 K. d) Thermal response measurements of CO_2 adsorption/desorption (1 bar, 298 K) of the materials prepared at 500 °C.

The CO_2 adsorption kinetics of the 350 °C samples are poor, and weak hysteresis is observed. At least CO_2 at room temperature can reach some of the internal pores while N_2 cannot. Taking this into consideration, it can be concluded that the "real" (equilibrium) selectivity of these samples might be higher, and that such polymer structures do indeed offer the possibility of CO_2 molecular sieving. Due to the presence of larger pores, the 500 °C samples show rapid equilibration as well as a sufficient selectivity reaching 50 for GU13-500, making them promising for CO_2 capture under relevant conditions (e.g., for removal of CO_2 from flue gas). It is interesting to note that while nitrogen sorption at liquid nitrogen temperatures decreases with increasing urea content, it is opposite for the CO_2 sorption at 273 K, i.e. the higher urea content in synthesis indeed promoted the formation of smaller micropores with dense heteroatom lining and induces specific adsorption sites for CO_2. The strength of the interaction between adsorbed CO_2 molecules and the surface of our materials can be estimated by calculating the isosteric heat of CO_2 adsorption (Q_{st}) using the Clausius-Clapeyron equation. With that, we calculated an apparent Q_{st} for the 500°C samples (assuming kinetic equilibrium for all cases) from the CO_2 adsorption isotherm measured at 273K (Fig. 4b) and 300 K (Fig. S12). The plot of the Q_{st} as a function of CO_2 uptake is shown in Fig. S13. Among the 500 °C samples, the most nitrogen-rich structure GU13-500 have the highest apparent Q_{st}, which ranges from 47 to 42 KJ mol^{-1} for the strongest binding sites. The Q_{st} values reported here are higher than those of most of previously reported porous carbon materials, especially activated carbons, but even with nitrogen heteroatoms present.[27] The high Q_{st} is clearly not only due to the pore size, but we assume that also the 1,4-para dual heteroatom doping does play a crucial role. Slightly higher Q_{st} values for CO_2 adsorption are only reported for some strongly polarizing metal-organic frameworks, specially modified zeolites, or nitrogen-doped microporous carbons functionalized with extra framework alkali metal cations.[2a, 11a, 28]

InfraSORP[29] measurements with CO_2 as the test gas at constant flow of 80 mL/min further visualize the structural properties of the 500 °C samples and their kinetic adsorption behavior (Fig. 4d). Noteworthy, the CO_2 diffusion in 500 °C samples is very fast as indicated by the nearly symmetric adsorption and desorption signals as well as the large and sharp temperature increase throughout cycling. In spite of the predominant microporous character, adsorption and desorption times are between 20 and 40 s. Accordingly, thermal response measurements of the 500 °C carbons show mass- related thermal response peak areas between 5.4 and 9.6 mg^{-1} (Fig. S14). This further indicates that the most structured GU13-500 sample has the very strong affinity and high binding enthalpy to CO_2, especially in the view of its relatively lower nitrogen surface area. The here described surface modifications thereby provide high CO_2 adsorption capacity, a high CO_2/N_2 selectivity, a high adsorption strength, and favorable adsorption kinetics.

Conclusions

In summary, we have developed a synthesis scheme based on gallic acid and urea to generate an assembled framework of heterocyclic rings forming a layered carbonaceous structure, however with about 30 wt% of heteroatoms, through directed condensation and ring closure. The unusually high content of heteroatoms (oxygen and nitrogen) can only be meaningfully assigned and included as phenazines, oxazine, or dioxine rings which inherit to the material high functionality and redox activity. Such a structure - when coupled to salt flux synthesis and templating – can be textured as a framework with high specific surface area with a practically completely heteroatom lining of the micropores. This method is simple, straightforward, sustainable by its starting products, and highly promising for scale up in an industrial environment. We believe that the newly described oxazoles and dioxine frameworks can be part of a rising library of functional tectons to access carbon-based materials with a wider range of properties, say for selective adsorption, as catalytic supports, or in electrocatalysis.

Conflicts of interest

There are no conflicts to declare.

Acknowledgements

The Max Planck Society is gratefully acknowledged for financial support. MA wants to thank the German Excellence UNICAT for continued support. We thank Regina Rothe for technical assistance and Ralf Walczak for the Ar and H_2O vapour physisorption tests. M.O. acknowledges financial support by a Liebig Fellowship of the German Chemical Industry Fund.

Zhihong Tian sincerely acknowledges the financial support provided by China Scholarship Council (CSC) of the Ministry of Education, P.R. China (No. 201707040019).

Notes and references

1 (a) X. Yu, Z. Tang, D. Sun, L. Ouyang and M. Zhu, *Prog. Mater. Sci.*, 2017, **88**, 1-48; (b) P. Puthiaraj, Y.-R. Lee and W.-S. Ahn, *Chem. Eng. J.*, 2017, **319**, 65-74; (c) J. S. M. Lee, M. E. Briggs, T. Hasell and A. I. Cooper, *Adv. Mater.*, 2016, **28**, 9804-9810; (d) T. S. Blankenship II, N. Balahmar and R. Mokaya, *Nat. Commun.*, 2017, **8**, 1545.

2 (a) M. Oschatz and M. Antonietti, *Energy Environ. Sci.*, 2018, **11**, 57-70; (b) Z. Tian, J. Huang, X. Zhang, G. Shao, Q. He, S. Cao and S. Yuan, *Micropor. Mesopor. Mat*, 2018, **257**, 19-26.

3 (a) A. Vasileff, Y. Zheng and S. Z. Qiao, *Adv. Energy Mater.*, 2017, **7**, 1700759; (b) Z. W. Seh, J. Kibsgaard, C. F. Dickens, I. Chorkendorff, J. K. Nørskov and T. F. Jaramillo, *Science*, 2017, **355**, 4998; (c) S. Liu, Z. Wang, S. Zhou, F. Yu, M. Yu, C. Y. Chiang, W. Zhou, J. Zhao and J. Qiu, *Adv. Mater.*, 2017, **29**, 1700874.

4 (a) X. Chen, R. Paul and L. Dai, *Natl. Sci. Rev.* 2017, **4**, 453-489; (b) C. Zhang, R. Kong, X. Wang, Y. Xu, F. Wang, W. Ren, Y. Wang, F. Su and J.-X. Jiang, *Carbon*, 2017, **114**, 608-618; (c) D. Zhu, Y. Wang, W. Lu, H. Zhang, Z. Song, D. Luo, L. Gan, M. Liu and D. Sun, *Carbon*, 2017, **111**, 667-674; (d) W. Li, S. Hu, X. Luo, Z. Li, X. Sun, M. Li, F. Liu and Y. Yu, *Adv. Mater.*, 2017, **29**, 1605820; (e) L. Borchardt, M. Oschatz and S. Kaskel, *Mater. Horiz.*, 2014, **1**, 157-168; (f) R. Yan, M. Antonietti, M. Oschatz. Adv. Energy Mater., 2018, **8**, 1800026.

5 (a) N. Fechler, N. P. Zussblatt, R. Rothe, R. Schlögl, M. G. Willinger, B. F. Chmelka and M. Antonietti, *Adv. Mater.*, 2016, **28**, 1287-1294; (b) T. Jordan, M. Shalom, M. Antonietti and N. Fechler, *Asia - Pac. J. Chem. Eng.*, 2016, **11**, 866-873.

6 (a) J. Mahmood, S.-M. Jung, S.-J. Kim, J. Park, J.-W. Yoo and J.-B. Baek, *Chem. Mater.*, 2015, **27**, 4860-4864; (b) J. Mahmood, E. K. Lee, M. Jung, D. Shin, I.-Y. Jeon, S.-M. Jung, H.-J. Choi, J.-M. Seo, S.-Y. Bae and S.-D. Sohn, *Nat. commun.*, 2015, **6**.

7 G. P. Hao, G. Mondin, Z. Zheng, T. Biemelt, S. Klosz, R. Schubel, A. Eychmüller and S. Kaskel, *Angew.Chem. Int .Ed.*, 2015, **54**, 1941-1945.

8 J. Xu, J. Zhu, X. Yang, S. Cao, J. Yu, M. Shalom and M. Antonietti, *Adv. Mater.*, 2016, **28**, 6727-6733.

9 L. Li, Y. Zhao, M. Antonietti and M. Shalom, *Small*, 2016, **12**, 6090-6097.

10 (a) J. Zhao, H. Lai, Z. Lyu, Y. Jiang, K. Xie, X. Wang, Q. Wu, L. Yang, Z. Jin and Y. Ma, *Adv. Mater.*, 2015, **27**, 3541-3545; (b) S. Porada, F. Schipper, M. Aslan, M. Antonietti, V. Presser and T. P. Fellinger, *ChemSusChem*, 2015, **8**, 1867-1874; (c) G.-P. Hao, Q. Zhang, M. Sin, F. Hippauf, L. Borchardt, E. Brunner and S. Kaskel, *Chem. Mater.*, 2016, **28**, 8715-8725.

11 (a) Y. Zhao, X. Liu, K. X. Yao, L. Zhao and Y. Han, *Chem. Mater.*, 2012, **24**, 4725-4734; (b) Y. Oh, V.-D. Le, U. N. Maiti, J. O. Hwang, W. J. Park, J. Lim, K. E. Lee, Y.-S. Bae, Y.-H. Kim and S. O. Kim, *ACS nano*, 2015, **9**, 9148-9157; (c) J. Gong, M. Antonietti and J. Yuan, *Angew. Chem.*, 2017, **129**, 7665-7671.

12 (a) W. Ju, A. Bagger, G.-P. Hao, A. S. Varela, I. Sinev, V. Bon, B. R. Cuenya, S. Kaskel, J. Rossmeisl and P. Strasser, *Nat. commun.*, 2017, **8**, 944; (b) H. Wang, S. Min, C. Ma, Z. Liu, W. Zhang, Q. Wang, D. Li, Y. Li, S. Turner and Y. Han, *Nat. Commun.*, 2017, **8**, 13592; (c) H. Wang, J. Jia, P. Song, Q. Wang, D. Li, S. Min, C. Qian, L. Wang, Y. F. Li and C. Ma, *Angew.Chem. Int .Ed.*, 2017, **56**, 7847-7852.

13 N. Fechler and M. Antonietti, *Nano Today*, 2015, **10**, 593-614.

14 M. Oschatz. M. Antonietti, *Adv. Mater.*, 2018, adma. 201706836R201706831.

15 (a) J. P. Paraknowitsch and A. Thomas, *Energ. Environ. Sci.*, 2013, **6**, 2839-2855; (b) H. Seema, K. C. Kemp, N. H. Le, S.-W. Park, V. Chandra, J. W. Lee and K. S. Kim, *Carbon*, 2014, **66**, 320-326.

16 Z. Xia, A. Singh, W. Kiratitanavit, R. Mosurkal, J. Kumar and R. Nagarajan, *Thermochim. Acta*, 2015, **605**, 77-85.

17 (a) L. Stradella and M. Argentero, *Thermochim. Acta*, 1993, **219**, 315-323; (b) W. Peng, W. Zhao, N. Zhao, J. Li, F. Xiao, W. Wei and Y. Sun, *Catal. Commun.*, 2008, **9**, 1219-1223.

18 (a) A.-A. G. Shaikh and S. Sivaram, *Chem. Rev.*, 1996, **96**, 951-976; (b) K. Sakaushi and M. Antonietti, *Accounts. Chem. Res.*, 2015, **48**, 1591-1600; (c) S. E. Denmark and G. L. Beutner, *Angew.Chem. Int .Ed.*, 2008, **47**, 1560-1638.

19 (a) T. Posner, *Lehrbuch der synthetischen Methoden der organischen Chemie*, Рипол Классик, 1903; (b) J. Morley, *Journal of the Chemical Society (Resumed)*, 1952, 4008-4014; (c) L. Kathawate, P. V. Joshi, T. K. Dash, S. Pal, M. Nikalje, T. Weyhermüller, V. G. Puranik, V. B. Konkimalla and S. Salunke-Gawali, *J. Mol. Struct.*, 2014, **1075**, 397-405.

20 Y. Chang, M. Antonietti and T. P. Fellinger, *Angew.Chem. Int .Ed.*, 2015, **54**, 5507-5512.

21 (a) S. Gadipelli, T. T. Zhao, S. A. Shevlin and Z. X. Guo, *Energy Environ. Sci.*, 2016, **9**, 1661-1667; (b) S. Gadipelli, Z. N. Li, T. T. Zhao, Y. C. Yang, T. Yildirim and Z. X. Guo, *J. Mater. Chem. A*, 2017, **5**, 24686-24694.

22 J. Lim, S. Y. Ryu, J. Kim and Y. Jun, *Nanoscale res. Let.*, 2013, **8**, 227.

23 S. Zhang, S. Tsuzuki, K. Ueno, K. Dokko and M. Watanabe, *Angew.Chem. Int .Ed.*, 2015, **54**, 1302-1306.

24 (a) A. Corma, *Chem. Rev.*, 1997, **97**, 2373-2420; (b) J. Pérez-Ramírez, C. H. Christensen, K. Egeblad, C. H. Christensen and J. C. Groen, *Chem. Soc. Rev.*, 2008, **37**, 2530-2542; (c) K. Na, C. Jo, J. Kim, K. Cho, J. Jung, Y. Seo, R. J. Messinger, B. F. Chmelka and R. Ryoo, *Science*, 2011, **333**, 328-332.

25 K. P. Gierszal, M. Jaroniec, T.-W. Kim, J. Kim and R. Ryoo, *New J. Chem.*, 2008, **32**, 981-993.

26 J. W. To, J. He, J. Mei, R. Haghpanah, Z. Chen, T. Kurosawa, S. Chen, W.-G. Bae, L. Pan and J. B.-H. Tok, *J. Am. Chem. Soc.*, 2016, **138**, 1001-1009.

27 X. Ren, H. Li, J. Chen, L. Wei, A. Modak, H. Yang and Q. Yang, *Carbon*, 2017, **114**, 473-481.

28 O. Shekhah, Y. Belmabkhout, Z. Chen, V. Guillerm, A. Cairns, K. Adil and M. Eddaoudi, *Nat. commun.*, 2014, **5**, 4228.

29 M. Oschatz, M. Leistner, W. Nickel and S. Kaskel, *Langmuir.*, 2015, **31**, 4040-4047.

View Article Online
DOI: 10.1039/C8TA03213K

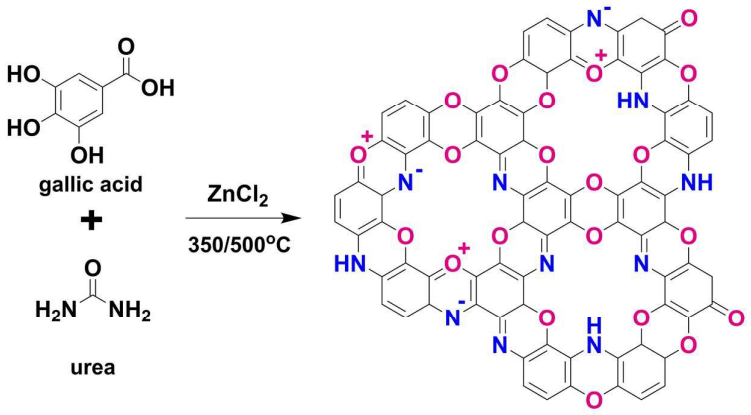

$C_2N_xO_{1-x}$ framework carbon with strongly polarizing structure and large specific surface area have been synthesized, which exhibit high affinity to CO_2.